

Slot Harmonic Effect on Magnetic Forces and Vibration in Low-Speed Permanent-Magnet Machine With Concentrated Windings

Mostafa Valavi, *Student Member, IEEE*, Arne Nysveen, *Senior Member, IEEE*, Robert Nilssen, and Terje Rølvåg

Abstract—In this paper, the influence of slot harmonics on magnetic forces and vibration is studied in a 120-slot/116-pole low-speed PM machine at no-load. It is shown how the lowest mode of vibration is produced at no-load due to slotting. Comparing the cases of open slots, semi-closed slots and magnetic wedges, the effect of slot closure on radial forces and torque production capability is discussed. Magnetic flux distribution in the airgap is computed using finite element analysis. Spatial harmonics due to slotting are investigated in different cases. Maxwell's stress tensor is employed to calculate radial and tangential components of the force density in the airgap. Spatial distribution of the total forces on the teeth and also time-dependent force waveform on one tooth are analyzed and discussed for different cases. It is shown how the magnitude of the lowest mode of vibration is reduced in the case of using semi-closed slots and magnetic wedges. Tangential force density distribution and torque production capability are also discussed. Structural analysis is presented to compute the maximum amplitude of the stator deformations due to the radial forces. Experimental results of the prototype generator are presented verifying the existence of the lowest mode of vibration at no-load because of the slot harmonics.

Index Terms—Electromagnetic forces, finite-element method, generators, permanent-magnet (PM) machines, vibration.

I. INTRODUCTION

PERMANENT-MAGNET (PM) machines with non-overlapping concentrated windings could potentially have more vibration problems than traditional PM machines. Radial force distribution in these machines contains low order harmonics leading to a higher vibration level [1]–[14]. Despite the problem of vibration and also relatively high rotor losses, PM machines with concentrated windings have been gaining popularity in several applications [15], [16]. Low cogging

Manuscript received November 29, 2013; accepted January 31, 2014. Date of publication March 4, 2014; date of current version September 16, 2014. Paper 2013-EMC-689, presented at the 2013 International Conference on Electrical Machines and Systems, Busan, Korea, October 26–29, and approved for publication in the IEEE TRANSACTIONS ON INDUSTRY APPLICATIONS by the Electric Machines Committee of the IEEE Industry Applications Society. This work was supported by the Norwegian Research Center for Offshore Wind Technology (NOWITECH).

M. Valavi, A. Nysveen, and R. Nilssen are with the Department of Electric Power Engineering, Norwegian University of Science and Technology, 7491 Trondheim, Norway (e-mail: mostafa.valavi@elkraft.ntnu.no; arne.nysveen@elkraft.ntnu.no; robert.nilssen@elkraft.ntnu.no).

T. Rølvåg is with the Department of Engineering Design and Materials, Norwegian University of Science and Technology, 7491 Trondheim, Norway (e-mail: terje.rolvag@ntnu.no).

Color versions of one or more of the figures in this paper are available online at <http://ieeexplore.ieee.org>.

Digital Object Identifier 10.1109/TIA.2014.2309717

torque, short end-windings and lower cost module level manufacturing are some of their advantages over traditional PM machines with distributed windings.

In low-speed PM machines (e.g., direct-driven wind generators) the outer diameter could be very large due to high number of poles. In this type of machines, using fractional slot concentrated windings topology could lead to a considerable reduction in size and weight. The reason is that it is possible to keep the number of slots as low as possible, as a result of a low q (i.e., number of slots per pole per phase). In this paper, radial magnetic forces and vibration are studied in a 120-slot/116-pole PM generator with single-layer concentrated windings.

Magnetic forces and vibration problems in PM machines with non-overlapping concentrated windings have been the subject of several research works in the last few years. A complete review of these works can be found in [1]. In [2], the authors discussed the vibration of PM brushless machines having a fractional number of slots per pole including both traditional and modular winding arrangements. It is pointed out that the modular 12-slot/10-pole machine has the highest vibration level. In [3], the magnetic forces on the stator teeth and resulting displacement are calculated for four different types of PM machines and it is shown that 12-slot/10-pole topology has the highest vibration level. In [4]–[6], it is shown that PM machines with concentrated windings are more susceptible to low frequency resonant vibrations. In [7], the radial magnetic forces and resulting displacement for a 30-slot/28-pole machine with concentrated windings are investigated and compared to 42-slot/28-pole and 84-slot/28-pole machines. In [8], the authors investigated the characteristics of the radial magnetic forces in a 12-slot/10-pole machine. In [9], the authors examined the radial forces and vibration in a 48-slot/44-pole machine. In [10], an analytical method is developed for analyzing the radial forces for fractional slot PM machines. In [11], radial forces and vibration modes of different PM machines are analyzed with different winding and rotor topologies. In [12], characteristics of the radial forces are presented for a 120-slot/116-pole generator with concentrated windings. In [13], influence of pole and slot combinations on radial forces and vibration is discussed in low-speed PM machines with concentrated windings.

The influence of slot harmonics on the characteristics of radial forces in fractional slot PM machines with concentrated windings is not well-covered in the mentioned literature where the rich harmonic content of the MMF (magnetomotive force)

TABLE I
PROTOTYPE GENERATOR SPECIFICATIONS

Rated power	30 kW
Number of phases	3
Rated frequency	50 Hz
Rated speed	51.7 rpm
Number of poles	116
Number of stator slots	120
Stator outer diameter	1777 mm
Stator material	M250-50A
Permanent magnets	NdFeB N35

has been identified as the main source of the vibration problems in fractional slot machines with concentrated windings. It means that it is not expected to see the lowest mode of vibration at no-load. The machines under investigation in the previous literature are mostly with semi-closed slots. This leads to reduce the effect of the slot harmonics significantly. It is worth mentioning that using open slots is a common practice in large PM machines with concentrated windings because of the manufacturing benefits. In this paper, the prototype machine has open slots and it is shown how slotting can produce the lowest mode of vibration even at no-load where there is no contribution from MMF harmonics. Slot harmonic effect in the prototype generator is discussed in Section II, where both slotless and slotted models are investigated using finite-element (FE) analysis at no-load. It is shown that lowest mode of vibration (4th spatial harmonic) only exists in the slotted machine. It can be concluded that the magnetic vibration at no-load is due to the slotting effect. In Section III, to investigate the influence of the slot closure on magnetic forces, different cases (i.e., open slots, semi-closed slots, and magnetic wedges) are modeled and studied using time-stepping FE analysis. The effect of slot closure on electromagnetic torque and eddy-current losses in rotor is also addressed in this section. Structural analysis of machines with open slots and magnetic wedges is also presented. Section IV includes experimental result of the prototype machine where the existence of the 4th mode of vibration is confirmed experimentally.

II. PROTOTYPE MACHINE WITH OPEN SLOTS

Prototype 120-slot/116-pole PM machine is a down-scaled low-speed wind generator [17]. It has open slots and single-layer concentrated windings. Specifications of the prototype generator are shown in Table I. Using open slots is common in large machines with concentrated windings mainly due to the distinct manufacturing advantages. In this section, influence of slot harmonics on distribution of flux density and force density in the prototype machine is investigated. Radial and tangential component of the magnetic flux density in the airgap at no-load are computed using magnetostatic FE analysis and then employed to calculate magnetic force density distribution.

A. Analysis of Flux Density

To study how the flux density distribution is distorted due to the slotting, a comparison between slotless and slotted cases

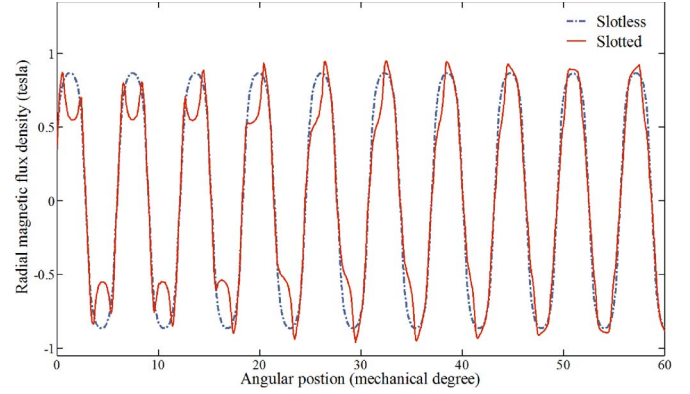


Fig. 1. Radial magnetic flux density in the airgap at no-load.

is made. Slotless model is a non-realistic case where slots are filled with the same material as stator teeth (i.e., laminated steel). Spatial distribution of the magnetic flux density in the airgap at no-load is depicted in Fig. 1 for both slotless and slotted cases. As it is evident in the figure, flux density is distorted in the slotted case and consequently new spatial harmonics (i.e., slot harmonics) are generated due to the slotting. At no-load, the field is produced only by the permanent magnets. Neglecting the slotting effect, the airgap radial and tangential magnetic flux density due to PMs can be written as [10]

$$B_r(\theta, t) = \sum_{n=1,3,5}^{\infty} B_{rn} \cos np(\theta - \omega t) \quad (1)$$

$$B_t(\theta, t) = \sum_{n=1,3,5}^{\infty} B_{tn} \sin np(\theta - \omega t) \quad (2)$$

where B_r and B_t represent the radial and tangential components of the magnetic flux density in the middle of the airgap. Angular mechanical position and velocity are denoted by θ and ω , respectively and p is the number of pole pairs. Hence, the spatial harmonic order for the radial field is np , where $n = 1, 3, 5, \dots$ and the tangential field has the same harmonic orders. Accordingly, the harmonic orders for no-load field in the slotless 120-slot/116-pole PM machine are 58, 174, 290, ... while the 58th (i.e., pole pair number) harmonic is the main component. In the slotted machine, the slot harmonics are also present in the magnetic field. Harmonic orders of the flux density in the slotted machine can be determined using the following equation [10]:

$$|np \pm iN_s| \quad (3)$$

where $n = 1, 3, 5, \dots$ and $i = 0, 1, 2, \dots$. N_s is the number of stator slots. Spatial harmonics generated in the slotted case can be seen in Fig. 2 where a comparison between slotless and slotted machines is presented. Fig. 3 shows the harmonic content of the flux density in the prototype 120-slot/116-pole machine which has open slots. From vibration point of view, the most important slot harmonic is $N_s - p = 62^{\text{th}}$ component. As will be discussed later, this slot harmonic plays a major role in generation of the lowest mode of vibration at no-load.

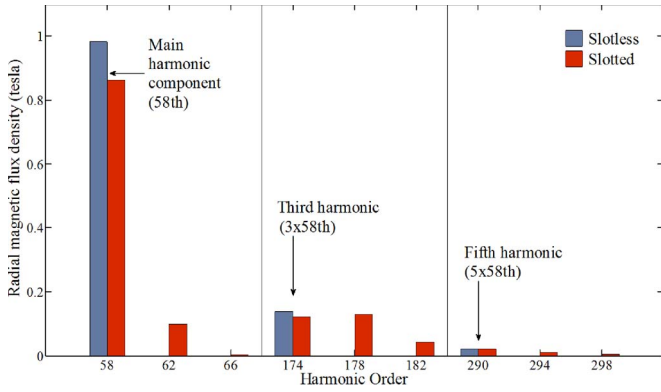


Fig. 2. Spatial harmonic orders of radial magnetic flux density in the airgap at no-load.

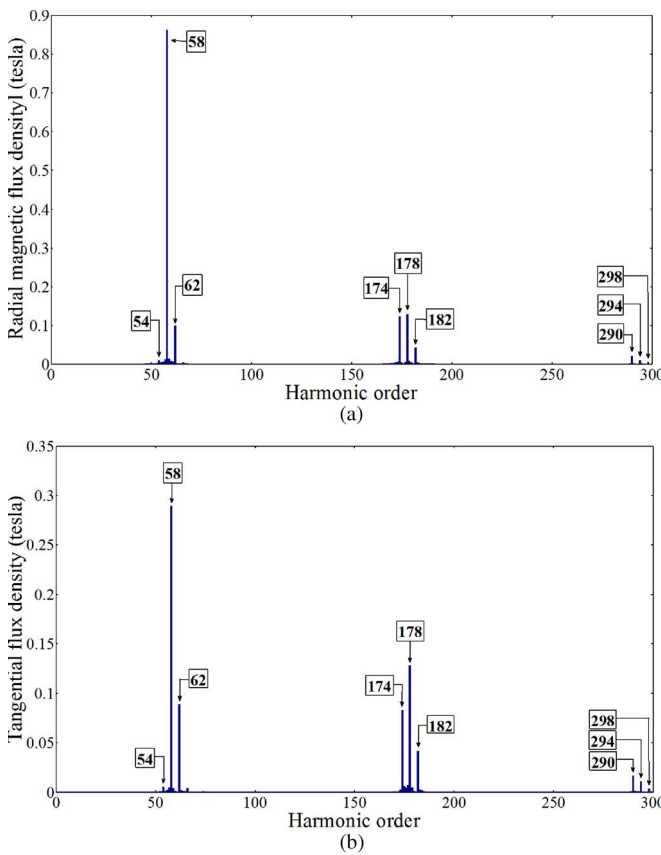


Fig. 3. Spatial harmonic distribution of magnetic flux density in the airgap in no-load. (a) Radial component. (b) Tangential component.

B. Analysis of Force Density

Radial magnetic forces are the main excitation for the magnetic vibration. Maxwell’s stress tensor is employed to calculate magnetic force density

$$f_r = \frac{1}{2\mu_0} (B_r^2 - B_t^2) \tag{4}$$

$$f_t = \frac{1}{\mu_0} (B_r B_t) \tag{5}$$

where f_r and f_t denote the radial and tangential components of the force density, respectively. The tangential component of

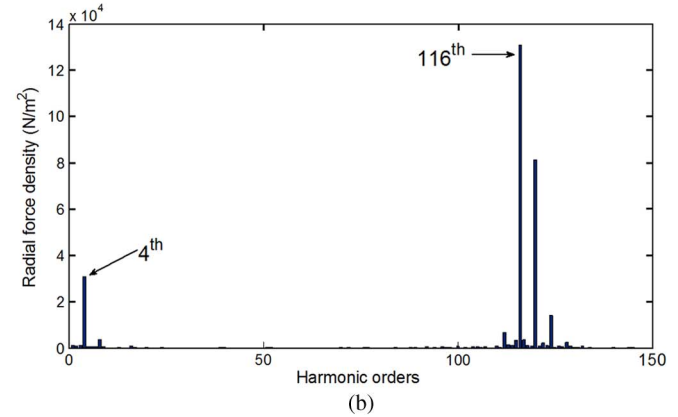
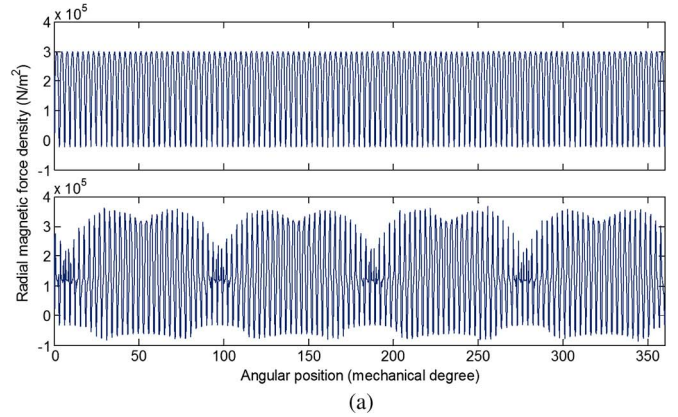


Fig. 4. (a) Radial magnetic forces in the airgap at no-load in slotless (top) and slotted machines (bottom). (b) Harmonic orders of radial force density for the prototype slotted machine at no-load.

force creates useful electromagnetic torque whereas radial component may cause undesirable vibration. The radial magnetic force density in the airgap can be expressed in the following general form:

$$f_r(\theta, t) = f_{r,max} \cos(m\theta - k\omega t) \tag{6}$$

where k is the time harmonic order and m represents the mode number. The radial forces cause deformations in the stator bore. The deformation amplitude is inversely proportional to m^4 [13]. Hence, the most critical mode is the lowest mode. The level of the magnetic vibration of the machine is mainly determined by this lowest mode of vibration [13]. Higher magnitude of the lowest mode leads to a higher level of magnetic vibration. In PM machines, the order of the lowest mode of vibration is equal to the greatest common divider (GCD) of number of slots and number of poles (i.e., 4 in the prototype machine).

Distribution of the radial magnetic forces is shown in Fig. 4 for both slotless and slotted cases. As can be seen in the figure, there is a strong spatial 4th force harmonic in the slotted case which is not present in the slotless case. Harmonic content of the radial force density in the slotted prototype machine is presented in Fig. 4(b). The 4th harmonic is the lowest harmonic order in the radial force density and has a considerable magnitude.

Lowest mode of vibration (i.e., 4th harmonic of force density) has a considerable magnitude even at no-load and is produced as a result of having open slots. It is important to

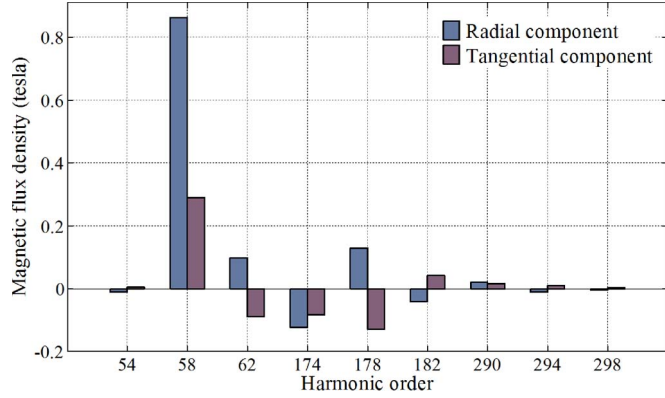


Fig. 5. Harmonic components of radial and tangential flux density in the airgap at no-load.

investigate how different harmonic pairs (i and j harmonic orders given by $i - j = 4$) in flux density contribute to produce lowest vibration mode. The key harmonic components in magnetic flux density distribution are shown in Fig. 3. In the following part, a harmonic analysis is carried out to clarify the production of the 4th harmonic order of radial forces in the prototype PM generator. Radial component of force density, according to (4), can be written as

$$f_r = f_{rr} - f_{rt} = \left(\frac{1}{2\mu_0} B_r^2 \right) - \left(\frac{1}{2\mu_0} B_t^2 \right) \quad (7)$$

where f_{rr} and f_{rt} are contributions from radial and tangential components of flux density, respectively. The radial force component produced by radial flux density can be written as

$$f_{rr} = \frac{1}{2\mu_0} \left[\sum_{k=1,2,3}^{\infty} B_{rk} \cos(k\theta) \right]^2 \quad (8)$$

where k is the spatial harmonic order and B_{rk} is the amplitude of the k th radial flux harmonic considering slotting effects. It is assumed that $\omega t = 0$. The 4th spatial harmonic in f_{rr} can be calculated as following:

$$f_{rr}(4^{th}) = \frac{1}{2\mu_0} \left[\frac{1}{2} B_{r2}^2 + \sum_{k=1,2,3}^{\infty} B_{rk} \cdot B_{r(k+4)} \right] \cos 4\theta. \quad (9)$$

According to Fig. 3(a), a few harmonic components have relatively large amplitude and need to be considered in the equation above. Therefore, the amplitude of the 4th harmonic order in (9) can be simplified as

$$f_{rr}(4^{th}) = \frac{1}{2\mu_0} (B_{r54}B_{r58} + B_{r58}B_{r62} + B_{r174}B_{r178} + B_{r178}B_{r182} + B_{r290}B_{r294} + B_{r294}B_{r298}). \quad (10)$$

In the equation above, in addition to amplitude, the sign of the harmonic component has a significant effect in the resulting amplitude of the force component. As can be seen in Fig. 5, amplitude of 58th, 62th, and 290th harmonic components is

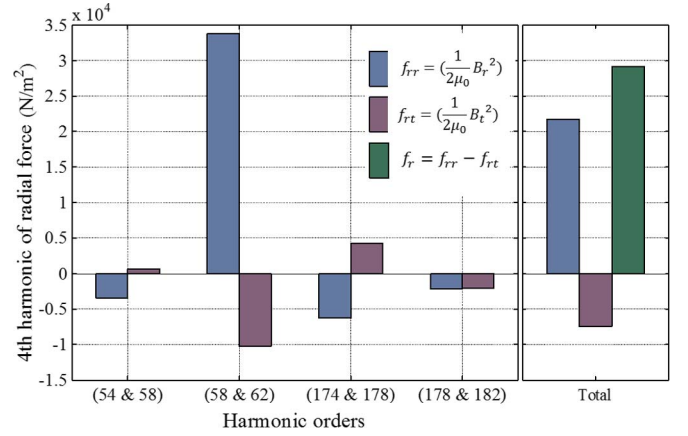


Fig. 6. Contribution of different flux density harmonics to produce 4th harmonic order in radial force distribution.

positive and the other harmonic components mentioned in (10) have negative amplitudes. The contribution of different harmonic pairs to produce 4th harmonic of f_{rr} is presented in Fig. 6. Influence of 290th, 294th, and 298th harmonics is very small and negligible. As can be seen in the figure, only $B_{r58}B_{r62}$ is positive and the other harmonic pair products reduce the amplitude of the resulting force component. So it can be said that interaction between 58th (main component) and 62th harmonics is the main factor in producing 4th harmonic component of f_{rr} .

The radial force component produced by tangential flux density can be analyzed in the same way. It can be written as

$$f_{rt} = \frac{1}{2\mu_0} \left[\sum_{k=1,2,3}^{\infty} B_{tk} \sin(k\theta) \right]^2 \quad (11)$$

where B_{tk} is the amplitude of the k th tangential flux harmonic considering slotting effects. It can be shown that the 4th harmonic component in f_{rt} can be written as

$$f_{rt}(4^{th}) = \left[\frac{1}{2\mu_0} \sum_{k=1,2,3}^{\infty} B_{tk} \cdot B_{t(k+4)} \right] \cos 4\theta. \quad (12)$$

According to Fig. 3(b) and similar to (10), the amplitude of the 4th harmonic in f_{rt} can be calculated as

$$F_{rt}(4^{th}) = \frac{1}{2\mu_0} (B_{t54}B_{t58} + B_{t58}B_{t62} + B_{t174}B_{t178} + B_{t178}B_{t182} + B_{t290}B_{t294} + B_{t294}B_{t298}). \quad (13)$$

Fig. 5 shows the sign of different harmonics in the tangential flux density. Here, in contrast to the radial flux density distribution, 62th harmonic is negative. The contribution of different harmonic pairs to produce 4th harmonic of f_{rt} is shown in Fig. 6. Due to a negative 62th harmonic, $B_{t58}B_{t62}$ is negative.

As can be seen in Fig. 6, contribution from 58th (main component) and 62nd harmonics is the main factor in production of the lowest mode of vibration. Relatively large positive f_{rr} and negative f_{rt} produced by this harmonic pair build up a

strong 4th harmonic in radial force density. There is almost no contribution from 178th and 182nd harmonic pair since f_{rr} and f_{rt} are almost equal. Interestingly, two other harmonic pairs (i.e., 54th and 58th, 174th and 178th) tend to reduce the magnitude of the lowest mode of vibration. If just the main harmonic pair (i.e., 58th and 62nd) is considered, the magnitude of 4th force harmonic would be 1.5 times the existing value where the contributions of other harmonic pairs are also considered. Significance of considering the contribution of tangential force density (i.e., f_{rt}) to produce lowest mode of vibration is evident in Fig. 6. According to the figure, 25% of the magnitude of the 4th spatial force harmonic is produced by f_{rt} .

In this paper, magnetic forces and vibration are investigated in a large low-speed PM machine whereas the focus of the previous research works has been mainly on small fractional slot machines (e.g., 12-slot/10-pole). Slot opening is usually narrow in those small machines leading to insignificant slot harmonic effects. The prototype 120-slot/116-pole machine under investigation has open slots and slotting effect on magnetic force distribution is substantial. In comparison between these two cases, the following should be noted.

- 1) In semi-closed small fractional slot machine with narrow slot opening, there is no major slot harmonic effect. As a result, it is addressed that lowest mode of vibration is not present at no-load and is produced by MMF harmonics [10]. In contrast, in the prototype machine due to open slots and considerable slot harmonic effect, a strong lowest mode of vibration exists even at no-load.
- 2) As will be discussed later in this paper, tangential component of flux density is larger in machines with wider slot openings. Consequently, the contribution of tangential flux density in production of force harmonics is more significant in machines with open slots. In the prototype machine under investigation, the importance of considering f_{rt} is emphasized. In contrast, in small fractional slot machines with narrow slot opening, it is addressed that f_{rt} can be neglected [10].

Summarizing two mentioned facts, in low-speed PM machines with non-overlapping concentrated windings and open slots, slot harmonic effect is significant. Consequently, lowest mode of vibration exists even at no-load and tangential flux density could not be neglected in the calculation of the radial magnetic forces.

III. INFLUENCE OF SLOT CLOSURE

Slot harmonic effect can be reduced through the use of semi-closed slots or magnetic wedges. In this section, using time-stepping FE analysis, radial and tangential forces are investigated and compared in four cases:

- 1) open slots;
- 2) magnetic wedge 1 ($\mu_r = 5$);
- 3) magnetic wedge 2 ($\mu_r = 10$);
- 4) semi-closed slots.

The first case (i.e., open slot) is the prototype PM generator. The other cases are identical to the prototype machine except in the slot closure. In the case of semi-closed slots, the slot opening is reduced by 50% compared to open slots. Two other

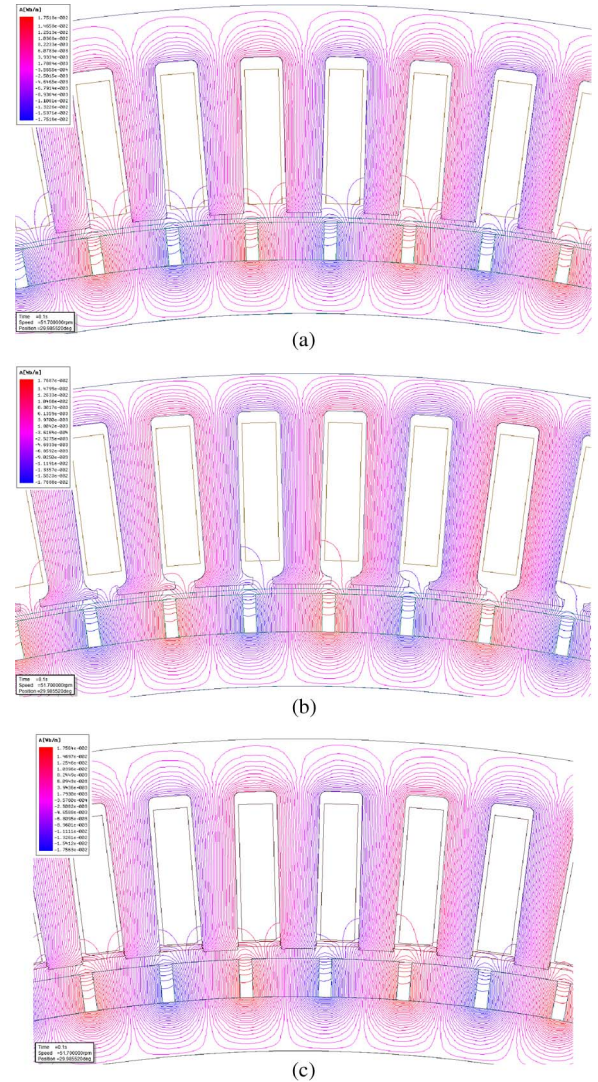


Fig. 7. Flux lines at no-load. (a) Open slots. (b) Semi-closed slots. (c) Magnetic wedges type 1.

cases are modeled with magnetic wedges, having $\mu_r = 5$ and $\mu_r = 10$ as relative permeability. Geometrical details about the mentioned cases as well as flux lines at no-load can be seen in Fig. 7.

A. Analysis of Flux Density

The radial and tangential components of the magnetic flux density in the airgap are computed using time-stepping FE analysis. The main component (i.e., 58th) and the most influential slot harmonic (i.e., 62nd) of radial flux density in the airgap are compared in Table II for four different cases. The main harmonic of tangential flux density (i.e., 58th) is also compared. According to the table, open slot and semi-closed slot cases have the lowest and highest values of main harmonic in radial flux density, respectively. Using magnetic wedges leads to a higher value of radial flux density in the airgap compared to open slots. Results show that in the case of magnetic wedge 2 ($\mu_r = 10$), the radial component of flux density is slightly larger compared to the case of magnetic wedge 1 ($\mu_r = 5$). From vibration point of view, the most important harmonic

TABLE II
AIRGAP FLUX DENSITY (TESLA)

	Open slot	Magnetic wedge 1 ($\mu_r=5$)	Magnetic wedge 2 ($\mu_r=10$)	Semi-closed slot
Radial component (main harmonic)	0.863	0.895	0.906	0.947
Radial component (62 nd harmonic)	0.095	0.067	0.058	0.0324
Tangential component (main harmonic)	0.284	0.254	0.245	0.2

TABLE III
RADIAL FORCE DENSITY (N/m^2)

	Open slot	Magnetic wedge 1 ($\mu_r=5$)	Magnetic wedge 2 ($\mu_r=10$)	Semi-closed slot
4 th harmonic	3.08×10^4	2.25×10^4	1.94×10^4	0.89×10^4
Mean value	1.33×10^5	1.47×10^5	1.52×10^5	1.73×10^5

in flux density distribution is the 62nd harmonic. Larger 62nd harmonic could lead to a larger lowest mode of vibration. Because it is the main contributor for generating the 4th spatial force harmonic as shown in Fig. 6. According to the table, 62nd harmonic is smallest in the case of the semi-closed slots and largest when open slots are used. This result is expected since any modification to reduce the rate of change of the permeance in the airgap reduces the harmonic content of the flux density. The amplitude of 62nd harmonic is reduced by 66% when semi-closed slots are used instead of the open slots. When magnetic wedges of type 1 and 2 are added to open slots, the amplitude of 62nd harmonic is also reduced by 29% and 39%, respectively. It is important to note that the main harmonic of the tangential flux density which contributes to produce useful electromagnetic torque is also heavily affected by the slot closure. As illustrated in the Table II, the main harmonic of tangential flux density is largest in the case of open slot. Together with manufacturing advantages, this is a benefit of using open slots. Modifications used to reduce slotting effects in the machine (i.e., using semi-closed slots or magnetic wedges) increase the radial component and reduce the tangential component of flux density in the airgap.

B. Radial Magnetic Forces

As mentioned before, in magnetic vibration of the electrical machine, the dominant vibration mode is the lowest-order harmonic in the radial force density distribution. Comparison of the lowest mode in the radial force spatial distribution in different cases can be used for comparison of the vibration level.

Time-stepping FE analysis is employed to compute magnetic flux density distribution in the airgap and then the results are used for calculation of magnetic forces according to (4) and (5). Table III compares the amplitude of the 4th spatial harmonic and mean value of radial force density for different cases. The amplitude of the 4th harmonic can be used to compare vibration levels. According to the table, by using semi-closed slots this

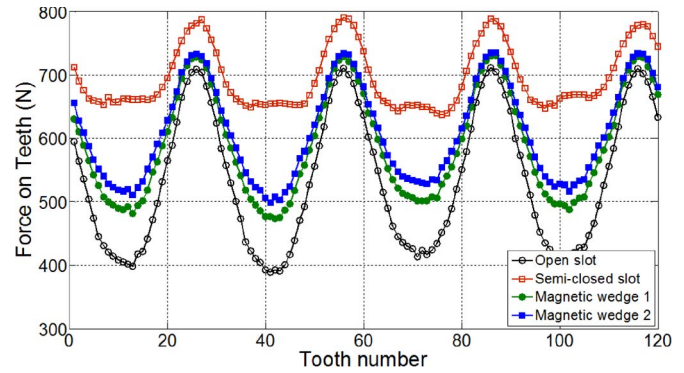


Fig. 8. Total forces on teeth in no-load.

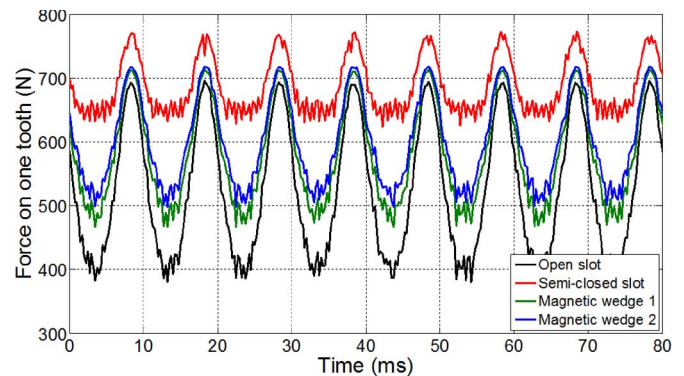


Fig. 9. Time-dependent force waveforms on one tooth in no-load.

TABLE IV
TIME-DEPENDENT FORCE ON ONE TOOTH (NEWTON)

	Open slot	Magnetic wedge 1 ($\mu_r=5$)	Magnetic wedge 2 ($\mu_r=10$)	Semi-closed slot
Peak-peak value	288	220	196	112
Mean value	525	582	604	687

amplitude is reduced by 71% leading to a large reduction in deformation amplitude. In the case of using magnetic wedges of type 1 and 2, the amplitude of 4th force harmonic is also reduced by 27% and 37%, respectively. Comparing Tables II and III, it is worth mentioning that the amount of reduction in the amplitude of the lowest mode of vibration is similar to the amount of reductions in the value of $B_{r58} \times B_{r62}$ and the magnitude of the 62nd harmonic in flux density. This illustrates the effect of slot harmonics and also direct contribution of the 62nd harmonic to generate the 4th harmonic in the force distribution. In addition to the 4th harmonic, the mean values of radial force density are presented in the table. There is a direct link between the amplitude of the main harmonic in the radial flux density and the mean value of the radial force density. As expected, the mean value is largest for semi-closed slots and smallest for the open slots.

Total force on each tooth can be calculated using a line integral over the tooth in the airgap. Total forces acting on all 120 teeth in one time step at no-load are depicted in Fig. 8. The presence of the 4th spatial mode is evident in all cases.

TABLE V
TANGENTIAL FORCES AND TORQUE (RESISTIVE LOAD)

	Open slot	Magnetic wedge 1 ($\mu_r=5$)	Magnetic wedge 2 ($\mu_r=10$)	Semi-closed slot
Mean value of tangential force density (N/m^2)	13.11×10^3	13.49×10^3	11.18×10^3	11.72×10^3
Mean value of torque in steady state ($kN.m$)	5.87	5.93	4.98	5.27

The obtained results shown in Table II regarding the amplitude of the 4th harmonic and mean values are also visualized in the Fig. 8.

Time-dependent total forces on one tooth for all four cases are shown in Fig. 9. The calculated values of the peak-peak and mean values of the forces are presented in Table IV. According to the table, the peak-peak value of force waveform is largest in open slots and smallest in semi-closed slots. The peak-peak value is reduced by 61% in semi-closed slots compared to the open slots. As mentioned before, because of the manufacturing difficulties, it is preferred not to use semi-closed slots in large machines. However, magnetic wedges can easily be used and according to the Table IV, the force peak to peak value is reduced by 24% and 32% for the type 1 and 2, respectively. Using wedges with higher permeability can lead to greater reduction in force variations and resulting vibrations. As can be seen in the Table IV, the mean value of the force is smallest for the open slots because the amplitude of main harmonic in radial flux density is smallest compared to the other cases.

C. Electromagnetic Torque

Since both radial and tangential components of the magnetic flux density in the airgap are affected by the slot closure, torque production capability is also expected to vary. To investigate the effect of the slot closure on the torque value in the steady state condition, time stepping FE analysis is performed for all four cases while machines are in the generator mode supplying a resistive load. A coupled circuit with FE simulations is used to model loading condition. The load characteristics are the same for all the four cases.

Average value of the torque is related to the mean value of the tangential force in load condition. According to Table II, both B_r and B_t are affected by the slot closure. As a result, the mean value of f_t also changes and consequently the average value of the produced torque changes. Table V presents the mean value of tangential force density and average torque for different cases of slot closure. Based on the presented results, in the case of the semi-closed slots, both average values of tangential force density and electromagnetic torque reduce by around 10% compared to the case of the open slots. The reduction of the torque is more significant in the case of using magnetic wedge 2 ($\mu_r = 10$) where a drop of around 15% can be seen in the average tangential force density and torque. Interestingly, when magnetic wedges 1 ($\mu_r = 5$) are used, the electromagnetic torque increases slightly compared to the case of open slots. The same pattern can be seen in the mean value of the tangential force density. Steady state torque waveforms are depicted in Fig. 10 for different cases. As can be seen in the

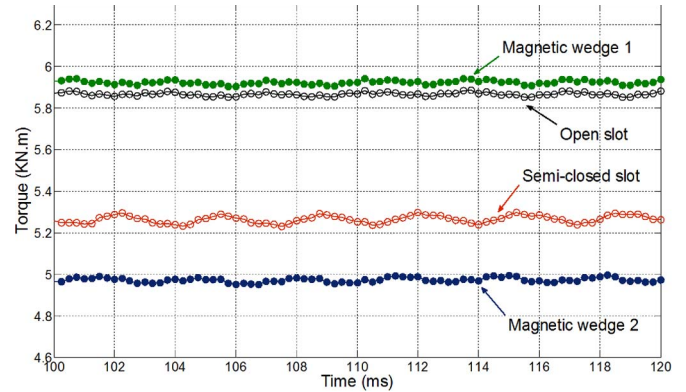


Fig. 10. Steady state torque waveforms (resistive load).

figure, machines with magnetic wedge 1 and 2 have the highest and lowest torque value, respectively.

D. Rotor Losses

Spatial harmonics produced by the slotting increase the eddy-current losses in the rotor. In the machines under investigation, the rotor back-iron is made of the solid steel and not laminations. Losses are computed using FE analysis and no analytical approach is employed. The total losses in rotor (permanent magnets and back-iron) for different cases are presented in Table VI for the no-load condition. As expected, losses are largest in the case of open slots since the slot harmonic effect is more significant. The rotor losses are reduced substantially in the case of semi-closed slots and magnetic wedges. The PM machine with semi-closed slots has the lowest losses.

E. Structural Analysis

To compute the stator deformations caused by the radial magnetic forces, static structural analysis is used. Deformations are compared in two cases: open slots and magnetic wedge 1. In order to calculate the natural frequencies and compute the stator deformation accurately, a 3-D structural model has to be employed including supporting structure and other mechanical details. A detailed structural analysis of the prototype PM machine (i.e., open slots) is presented in [13].

In this paper, to show the distinct differences in the deformations caused by different exciting magnetic forces, the structural supports have not been considered in the structural analysis. The reason is that those supports could significantly damp the magnitude of the resulting deformations. The difference between two cases (i.e., open slots and magnetic wedge 1) is clearer when only the stator is considered in the structural model. However, it is worth mentioning that if the supporting

TABLE VI
ROTOR LOSSES AT NO-LOAD

	Open slot	Magnetic wedge 1 ($\mu_r=5$)	Magnetic wedge 2 ($\mu_r=10$)	Semi-closed slot
Losses in PMs and solid rotor (W)	440	225	165	50
Percentage of the output electrical power	1.57 %	0.79 %	0.70 %	0.20 %

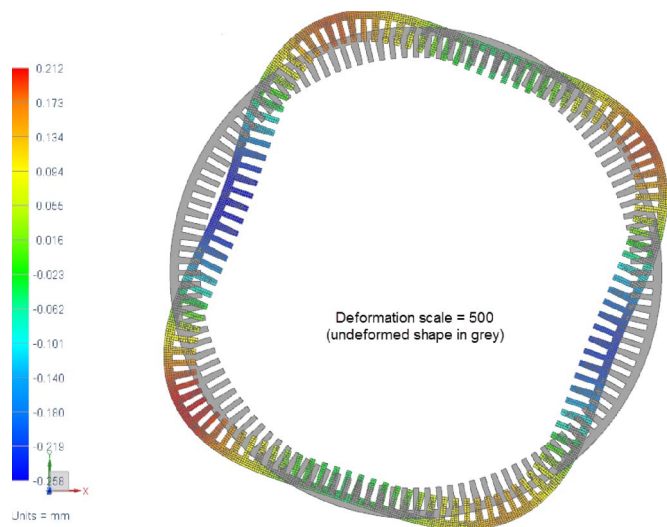


Fig. 11. Deformations caused by magnetic forces at no-load in prototype machine.

structure is also included in the analysis, the results are more realistic. Modal and static deformation analysis of the prototype machine including supporting structures can be found in [13], where calculated and measured results of the deformations are in good agreement.

Radial magnetic forces shown in Fig. 8 are used as exciting forces for structural analysis to compute deformations of stator bore. Average value of magnetic force does not cause vibration and the peak-peak value of force should be used as a basis for comparing the vibration level. Since the peak-peak value is reduced by 24% in the case of magnetic wedge 1 compared to the case of open slots, it is natural to have smaller deformations in the stator bore and consequently have a lower vibration level when the magnetic wedges are inserted in the slots. Results of the structural analysis verify that the stator bore experiences smaller deformations in the case of the magnetic wedge 1 ($\mu_r = 5$). In this case the magnitude of the deformations is reduced by 22% compared to the case of open slots. Fig. 11 shows the deformations in the prototype machine with open slots. The 4th spatial mode can be observed in the deformation pattern in the figure.

F. Discussion

According to Section III-B, the magnitude of the 4th spatial harmonic is lowest in the case of semi-closed slots meaning that the vibration level is also expected to be lowest. Rotor losses at no-load is also smallest when using semi-closed slots due to the reduced slot harmonic effect. However, according to Section III-C, the electromagnetic torque is reduced in this case

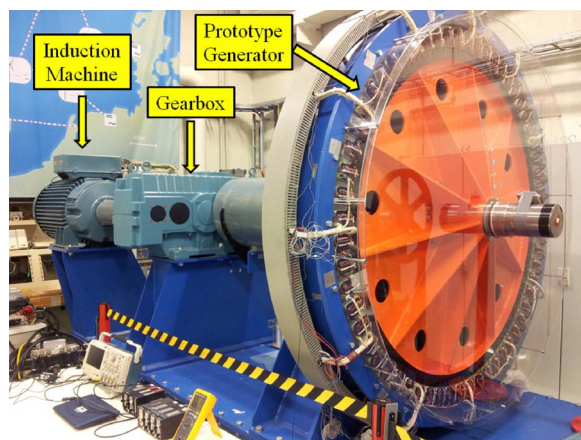


Fig. 12. Experimental setup.

which is a drawback. It is also worth noting that it is preferred not to use semi-closed slots in large PM machine since using open slots or magnetic wedges is more beneficial from a manufacturing point of view. As presented in Section III-B, using magnetic wedges leads to a lower vibration level and also lower rotor losses according to Section III-D. Larger value of the relative magnetic permeability ($\mu_r = 10$) leads to a lower magnitude of 4th spatial harmonic and lower losses but significantly lower produced torque. On the other hand, the PM machine having magnetic wedge 1 ($\mu_r = 5$) has a reduced vibration level (reduced magnitude of 4th spatial harmonic), reduced rotor losses and also slightly higher torque compared to the prototype machine with open slots. Using magnetic wedge 1 can improve vibration and loss characteristics of the machine while the torque production capability is not affected in a negative way. This suggests that it is possible to choose a proper value of the μ_r for the magnetic wedges to improve machine performance.

IV. EXPERIMENTAL RESULTS

Experimental work is carried out to verify that there is a 4th mode of vibration present in the prototype machine even at no-load, due to slotting. As mentioned before, this 4th mode is generated mostly as a result of the interaction between 58th and 62nd spatial harmonics in magnetic flux density distribution. The experimental work of the prototype machine is comprehensively presented in [13] and this section covers a brief summary. The experimental setup is shown in Fig. 12.

To confirm the existence of the 4th mode at no-load, four accelerometers are mounted on the stator, as shown in Fig. 13. According to Fig. 8, these sensors should experience the same magnitude of the radial forces at all times. This means that the acceleration waveforms of all these four sensors have to be in

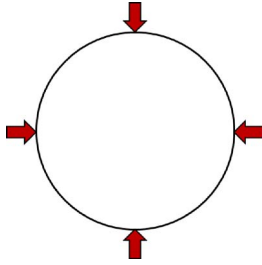


Fig. 13. Positioning of the accelerometers for mode observation.

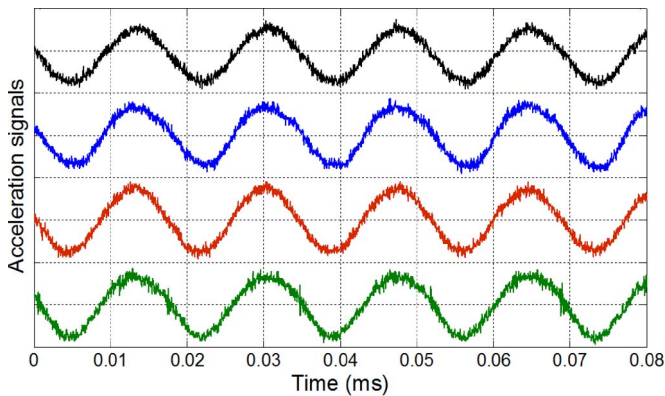


Fig. 14. Acceleration signals from four sensors [13].

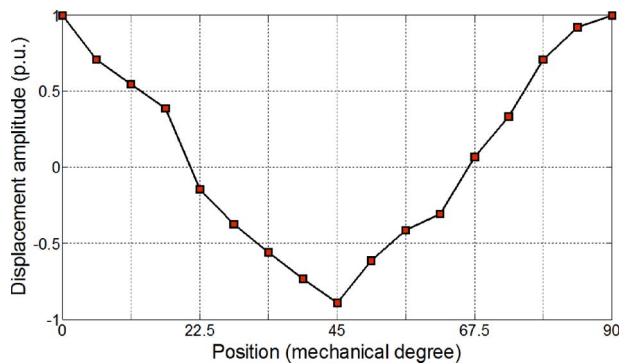


Fig. 15. Rough approximation of the spatial distribution of displacement amplitude [13].

phase if there is a 4th mode of vibration. The acceleration waveforms are shown in Fig. 14. It is evident that all acceleration signals are in phase. To visualize a quarter of the 4th spatial mode shape, two sensors are fixed 90° apart and a third sensor is moved from one of the fixed sensors toward another one. Using the phase shift between the acceleration signals at a number of points, a rough approximation of the spatial distribution of the displacements can be obtained. This waveform is depicted in Fig. 15 and clearly shows a quarter of the 4th spatial harmonic as expected according to Figs. 8 and 11.

V. CONCLUSION

In this paper, effects of slot harmonics on magnetic forces are investigated. Using FE analysis, a 120-slot/116-pole PM machine is modeled with different types of slot closure. It is shown how the lowest mode of vibration is produced at no-load due to slotting. Contribution of different spatial harmonics in

flux density to produce 4th spatial harmonic of radial forces is investigated. Effect of slot closure on the magnitude of the harmonics in flux density distribution, lowest mode of vibration, rotor losses and electromagnetic torque is studied. It is shown the magnitude of the lowest mode of vibration is reduced in the case of using semi-closed slots or magnetic wedges leading to a lower vibration level. The lowest vibration level could be achieved using semi-closed slots. However, the produced torque is also reduced considerably. The torque production capability is also reduced even further if the magnetic wedge 2 ($\mu_r = 10$) is used. In the case of magnetic wedge 1 ($\mu_r = 5$), the magnitude of the 4th spatial mode of radial force density and the resulting vibration are reduced compared to the case of open slots. In addition, torque production capability is improved slightly.

REFERENCES

- [1] M. Valavi, A. Nysveen, and R. Nilssen, "Magnetic forces and vibration in permanent magnet machines with non-overlapping concentrated windings: A review," in *Proc. IEEE ICIT*, 2012, pp. 977–984.
- [2] Y. S. Chen, Z. Q. Zhu, and D. Howe, "Vibration of PM brushless machines having a fractional number of slots per pole," *IEEE Trans. Magn.*, vol. 42, no. 10, pp. 3395–3397, Oct. 2006.
- [3] R. Islam and I. Husain, "Analytical model for predicting noise and vibration in permanent-magnet synchronous motors," *IEEE Trans. Ind. Appl.*, vol. 46, no. 6, pp. 2346–2354, Nov./Dec. 2010.
- [4] J. Wang, Z. P. Xia, D. Howe, and S. A. Long, "Vibration characteristics of modular permanent magnet brushless AC machines," in *Conf. Rec. IEEE IAS Annu. Meeting*, 2006, pp. 1501–1506.
- [5] J. Wang, Z. P. Xia, S. A. Long, and D. Howe, "Radial force density and vibration characteristics of modular permanent magnet brushless AC machine," *Proc. Inst. Elect. Eng.—Elect. Power Appl.*, vol. 153, no. 6, pp. 793–801, Nov. 2006.
- [6] J. Wang, Z. P. Xia, D. Howe, and S. A. Long, "Comparative study of 3-phase permanent magnet brushless machines with concentrated, distributed and modular windings," in *Proc. IET Int. Conf. PEMD*, 2006, pp. 489–493.
- [7] H. C. M. Mai *et al.*, "Consideration of radial magnetic forces in brushless DC motors," in *Proc. ICEMS*, 2010, pp. 1–6.
- [8] Z. Q. Zhu, Z. P. Xia, L. J. Wu, and G. W. Jewell, "Influence of slot and pole number combination on radial force and vibration modes in fractional slot PM brushless machines having single- and double-layer windings," in *Proc. IEEE ECCE*, 2009, pp. 3443–3450.
- [9] A. Cassat *et al.*, "Forces and vibration analysis in industrial PM motors having concentric windings," in *Proc. IEEE ECCE*, 2010, pp. 2755–2762.
- [10] Z. Q. Zhu, Z. P. Xia, L. J. Wu, and G. W. Jewell, "Analytical modeling and finite-element computation of radial vibration force in fractional-slot permanent-magnet brushless machines," *IEEE Trans. Ind. Appl.*, vol. 46, no. 5, pp. 1908–1918, Sep./Oct. 2010.
- [11] G. Dajaku and D. Gerling, "The influence of permeance effect on the magnetic radial forces of permanent magnet synchronous machines," *IEEE Trans. Magn.*, vol. 49, no. 6, pp. 2953–2966, Jun. 2013.
- [12] M. Valavi, A. Nysveen, and R. Nilssen, "Characterization of radial magnetic forces in low-speed permanent magnet wind generator with non-overlapping concentrated windings," in *Proc. ICEM*, 2012, pp. 2943–2948.
- [13] M. Valavi, A. Nysveen, R. Nilssen, R. D. Lorenz, and T. Rølvåg, "Influence of pole and slot combinations on magnetic forces and vibration in low-speed PM wind generators," *IEEE Trans. Magn.*, vol. 50, no. 5, p. 8700111, May 2014.
- [14] F. Magnussen and H. Lendenmann, "Parasitic effects in PM machines with concentrated windings," *IEEE Trans. Ind. Appl.*, vol. 43, no. 5, pp. 1223–1232, Sep./Oct. 2007.
- [15] A. M. EL-Refaie, "Fractional-slot concentrated-windings synchronous permanent magnet machines: Opportunities and challenges," *IEEE Trans. Ind. Electron.*, vol. 57, no. 1, pp. 107–121, Jan. 2010.
- [16] A. M. EL-Refaie, "Fractional-slot concentrated-windings: A paradigm shift in electrical machines," in *Proc. IEEE WEMDCD*, 2013, pp. 24–32.
- [17] Ø. Krøvel, "Design of large permanent magnetized synchronous electric machines," Ph.D. dissertation, Norwegian Univ. Sci. Technol., Trondheim, Norway, 2011.



Mostafa Valavi (S'07) received the B.Sc. and M.Sc. degrees in electrical power engineering from the University of Tehran, Tehran, Iran, in 2007 and 2010, respectively. He is currently working toward the Ph.D. degree at the Norwegian University of Science and Technology, Trondheim, Norway.

His research interests include analysis and design of electrical machines.



Arne Nysveen (M'98–SM'06) was born in Hamar, Norway, in 1965. He received the M.Sc. degree in electrical power engineering and the Dr.Ing. degree from the Norwegian Institute of Technology (NTH), Trondheim, Norway, in 1988 and 1994, respectively.

From 1995 to 2002, he was a Research Scientist at ABB Corporate Research in Oslo, Norway. His main research dealt with subsea power supply and electrical power apparatus. Since 2002, he has been a Professor in the Faculty of Electrical Power Engineering at the Norwegian University of Science and

Technology (NTNU), Trondheim, Norway. He holds several patents on subsea power equipment and electric machinery.



Robert Nilssen received the M.Sc. and Dr.Ing. degrees from the Norwegian Institute of Technology (NTH), Trondheim, Norway, in 1983 and 1988, respectively, specializing in the field of finite-element analysis.

He was an Advisor to the Norwegian Research Institute of Energy Supply and SINTEF. He is currently a Professor of electrical engineering at the Norwegian University of Science and Technology (NTNU), Trondheim, Norway. His current research interests include the design of electromagnetic components and electrical machines, optimization, and modeling. He is a cofounder of several companies.

of several companies.



Terje Rølvåg was born in Mo i Rana, Norway, in 1963. He received the M.Sc. and Ph.D. degrees in finite-element dynamics of elastic mechanisms and control from the Norwegian Institute of Technology (NTH), Trondheim, Norway.

His working experience includes SINTEF Production Engineering, SINTEF Materials Technology, FEDEM Technology AS and TRAC, the latter in combination with an adjunct professorship in the Department of Engineering Design and Materials (IPM), NTNU. Since 2003, he has been a Professor

in the Engineering Design group at IPM.

His research interests cover computer science applied to engineering applications focusing on simulation of behavior and strength of electromechanical products.